COBEM 2021 26th International Congress of Mechanical Engineering
November 22-26, 2021, Virtual Congress, Brazil
ABCM Associação Brasileira de Engenharia e Ciências Mecânicas

COB-2021-0150
DESIGN AND CONSTRUCTION OF A DIDACTIC LOW-VELOCITY WIND TUNNEL

Arthur de Lima Queiroga
Aerospace Engineering Department, Faculty UnB Gama - FGA, University of Brasilia, Área Especial de Indústria Projeção A, Setor Leste, Gama, 72.444-240, Brasilia - Brazil
e-mail

Olexiy Shynkarenko
Aerospace Engineering Department - Chemical Propulsion Laboratory, Faculty UnB Gama - FGA, University of Brasilia, Área Especial de Indústria Projeção A, Setor Leste, Gama, 72.444-240, Brasilia - Brazil
olexiy@aerospace.unb.br

Rhander Viana
Automotive Engineering Department, Faculty UnB Gama - FGA, University of Brasilia, Área Especial de Indústria Projeção A, Setor Leste, Gama, 72.444-240, Brasilia - Brazil
e-mail

Abstract. *Experimental aerodynamics plays an essential role in the development of aerospace structures. It complements numerical simulations and analytical modeling. The primary tool in an empirical study of aerodynamic processes is the wind tunnel. This work's main objective is to design, build, and characterize a bench wind tunnel approximately 2.5 meters long and with preferentially laminar flow in its testing section. An open-circuit wind tunnel is a low-cost solution affordable by student research teams. Compared to other types, an open circuit system is smaller, simpler, and cheaper for manufacturing. The following parts compose the tunnel structure: a settling chamber, nozzle, test chamber, diffuser, and a power unit (ventilator). Air enters the settling chamber, where the honeycomb-type flow straightener improves its uniformity. The nozzle influences the flow quality in the test chamber. The nozzle geometry follows recommendations about contraction ratio, length, and shape. A fan with straight blades adds energy to the system. The numerical simulation based on incompressible transient Navier-Stokes equations studies turbulence and viscous effects in the tunnel. The structured three-dimensional mesh used in the simulation takes into account flow gradients. The SST turbulence model validated for low-velocity applications describes the propagation of the boundary layer. The boundary layer properties and especially laminar-turbulent transition in the tunnel are also studied numerically. Further building of the system will allow validating theoretical and numerical studies. The wind tunnel will enable studying pressure distribution on aerodynamic bodies' surface and low-velocity flow visualization using a smoke machine.*

Keywords: *wind tunnel, flow visualization, flow characterization, subsonic nozzle, wind tunnel design*

1. INTRODUCTION

Several areas utilize applied aerodynamics, such as construction (e.g., buildings and bridges), vehicles (e.g., automobiles and planes), special equipment (e.g., aero-generators and parachutes), among others. Since the 20th century, research in the aerodynamic domain was motivated mainly by the need to improve the performance and fuel consumption of cars and planes, especially when the car manufacturers found that cars lost power to the air drag (Mehta and Bradshaw, 1979). Research in the aerodynamic area evolved essentially with the development of wind tunnels. This equipment allows engineers to study the airflow over objects of interest, forces acting on them, and interaction with the flow. Researchers use wind tunnels to investigate aerodynamic theories and mainly facilitate aircraft design. Currently, aerodynamic experimentation has expanded into other fields such as the automotive industry, architecture, environment, and education, which makes low-speed tunnels relevant (Carminatti and Konrath, 2019). The practice of low-speed experimental aerodynamics was fundamental in developing many vehicles and other devices that must perform their functions in the presence of forces generated by air or water flows.

The study of aerodynamics provides a variety of ways to develop a product or experiment. The analysis in this field is achievable in three ways: analytical, computational, and experimental. In the past, humanity did not have access to modern computers. Therefore, only the analytical and experimental methods allowed us to understand fluids. An example of this is the Wright brothers, who, at the beginning of the 20th century, were one of the pioneers in the aeronautical field

(Anderson, 2016).

Computational studies gained significant importance in aerodynamics after developing powerful computers at the end of the 20th and the beginning of the 21st century, but experimental analyses were not left aside. Currently, wind tunnels carry out the validation of analytical and computational results. These structures are divided into two categories and have two possible test section configurations. The two types are open and closed circuits, and the test section can be open or closed.

In an open circuit tunnel, the air does not recirculate inside. Such a tunnel is usually cheaper and allows testing with internal combustion machinery. Unfortunately, this tunnel has some disadvantages. It is extremely noisy and sensitive to the environment. That is, the configuration of the room affects the flow in the tunnel. In this tube, the flow passes through a nozzle, a test section, a diffuser, and finally, the fan.

A closed-circuit wind tunnel is a much more complex structure where air recirculates inside it. As it has a closed circuit, it generates less noise and interference induced by the external environment. These tunnels have high efficiency because they use less energy to reach the proper speed in the test section. Closed-circuit tunnels provide good-quality flow but are much more expensive due to their structural complexity and because they need much space for installation (Barlow *et al.*, 1999).

The test section is open when it does not have solid barriers and closed when it has walls that delimit the test region. A wind tunnel with an open test section allows experiments with full-size or larger-scale structures, yielding more reliable results. The Langley Research Center, in Hampton, USA, has a wind tunnel with this type of test section.

The design of a wind tunnel has a relation to the final objective of the research, the investment capital, and the available space for the structure. Wind tunnels are adequate equipment for subsonic, transonic, and supersonic aerodynamic studies, as these types of equipment allow analyzing the fluid in its greatest complexity. The right tunnel type allows acquiring extremely relevant test data (Barlow *et al.*, 1999).

The main objective of this work is to design and build a bench wind tunnel, which preferably has a uniform flow in its test section. An open circuit with a closed test section is the chosen option. According to the literature, structural tunnel elements such as settling chamber, nozzle, diffuser, and test section are designed. The flow numerical simulation inside the tunnel validates its structure and flow behavior inside the test section.

2. METHODOLOGY

2.1 Structural Design

The project aims to design an open-circuit wind tunnel of approximately 2 meters long, reaching a speed of 9 m/s in the test section and allowing to visualize the flow behavior during experiments inside the test section.

2.1.1 Settling Chamber

The uniformization process of the flow starts in the settling chamber, reducing vorticities. Installation of a honeycomb plate in a constant-area inlet section makes the flow most laminar possible. This plate must follow three essential parameters for its design: the cell size, the cell wall thickness, and the honeycomb plate thickness.

Initially, the market analysis allowed us to find out the available honeycomb. Knowing the size of cells and their wall thickness makes it possible to calculate the surface area of the honeycomb. The thin cell walls provide an array of straight passageways with a 97% open area, which results in a small pressure drop and reduced turbulence and noise. Another critical factor is the cell size ratio to the core thickness. Cell size must be seven times or greater than the core thickness. Therefore, the cell cannot be too large because the honeycomb plate thickness would be too large. The large plate requires extra material, and thus this piece becomes more expensive (Bitzer, 1997).

2.1.2 Test Chamber

The test section is one of the starting points of a wind tunnel project, where the speed of the wind and flow quality are the two starting points for its design. This section carries out the experiments and allows us to observe the fluid behavior. The structure that best fits the wind tunnel specification is the square section. The length of the test section is twice its hydraulic diameter.

2.1.3 Power Unit

The fan as a power unit is a relevant structure for initial design considerations. Axial fans have predefined sizes and different types of blades. The developed wind tunnel utilizes a fan with straight blades, as recommended in the literature.

The authors estimated the fan power according to Barlow *et al.* (1999). There are two fans with different diameters in the catalog of axial ventilators for the stipulated power. The first ventilator has a diameter of 0.3 m, and the other one of 0.4 m. The fan supply is 12 V and two-phase. The fan speed control utilizes analog Pulse-Width Modulation (PWM).

Experimentally was found the fan speed using the tachometer and anemometer. After the flow velocity measurement, according to the Bernoulli equation, the dynamic pressure equals to

$$p_d = \frac{1}{2}\rho V^2 \tag{1}$$

2.1.4 Nozzle

The nozzle is a critical part of the design of a wind tunnel. It has a high impact on the test chamber flow quality. The construction of this part has to respect the following three parameters: area ratio, the angles $\alpha/2$ e $\beta/2$, and the shape. These angles are shown on the left and the shape on the right in Fig. 1.

For a wind tunnel with aeronautical purposes, a valid area ratio is between 8 and 9. In relation to the angles $\alpha/2$ and $\beta/2$ the recommended value is $12°$, according to Ahmed (2013). However, such a large area proportion increases the length of the nozzle. The following formula gives an estimation of the area ratio, where A_e is the inlet area of the flow and A_s is the outlet area.

$$N = \frac{A_e}{A_s} \tag{2}$$

The dimensions of the test section define the hydraulic diameter of the nozzle outlet. It is necessary to define the hydraulic inlet diameter. The size of this entry must respect the area ratio condition. With the inlet diameter value defining the nozzle length, L, it is found using the equation 3 where θ is $12°$, R_1 is half of the hydraulic inlet diameter and R_2 is half of the outlet hydraulic diameter.

$$\theta = arctan\left(\frac{R_2 - R_1}{L}\right) \tag{3}$$

Finally, this optimal nozzle geometry requires a definition of the hydraulic diameter and length. A straight nozzle would be the most straightforward and most economical option, but the flow inside the test section would not be satisfactory (Driss, 2019). Therefore, following the conclusions presented in the literature, we opted for a nozzle formed by two cubic equations, as shown in Fig. 1. This curved nozzle shape follows the work Zanoun (2018).

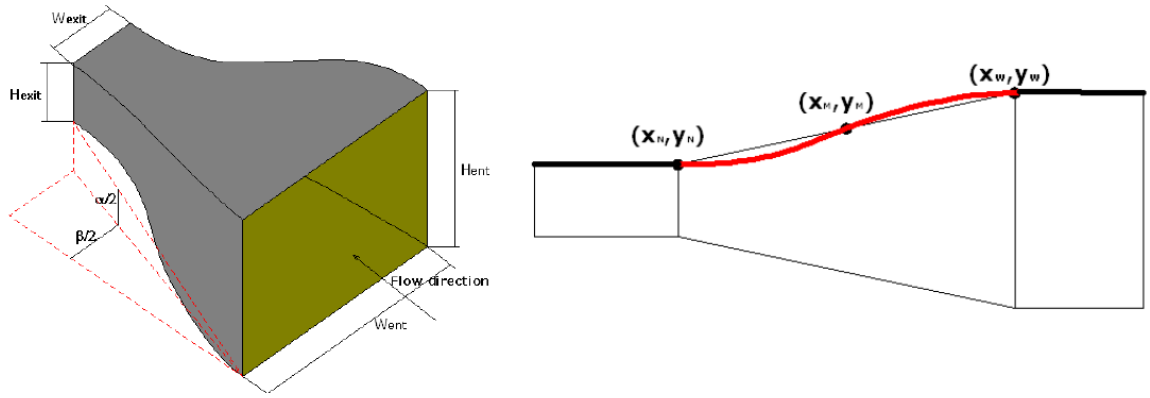

Figure 1. Nozzle layout, Ahmed (2013)

2.1.5 Difuser

This part is essential for the quality of the flow because if the boundary layer detaches, the pressure variations in this region will affect the flow in the test chamber. Two values of R_2 were chosen for analysis. They depend on the fan diameter. The length of the tunnel is a limiting factor for this design. A fan diameter of 0.4 m would make the diffuser too long. Thus, a 0.3 m diameter fan was chosen, which provides a good area ratio between the inlet and outlet, and also a good length for the project, using the equation 3. Then, the diffuser length for an expansion angle, θ of $3°$ Ahmed (2013).

2.2 Numerical simulation

The incompressible averaged Navier-Stokes equations approximate the physical processes in the low-velocity wind tunnel. Expressed in three-dimensional form Tannehill *et al.* (1997) together with $k-\omega$ SST model, this equation system perfectly describes the flow behavior in a computational domain according to Ansys (2020). The Ansys Fluent provides a solution to the equation system. The “pressure inlet” and “pressure outlet” type bounds define the boundary conditions

of the domain. Wall utilizes the non-slipping conditions (zero velocity on the wall) with the "Standard" roughness model. The Bernoulli equation predicts the initial flow velocity. The third-order MUSCL solution method for the flow equations and second-order upwind method with high order term relaxation for the turbulence properties allow receiving a high-quality simulation result.

The flow convergence accounting all the flow parameters with the absolute criteria of 0.001 usually occurs after 50 to 100 iterations. An analysis of the following parameters is necessary for a definitive study of the flow pattern in the aerodynamic wind tunnel: velocity change along the wind tunnel, the y^+ criteria, velocity uniformity and boundary layer behavior in the test section.

3. RESULTS

3.1 Tunnel Geometry

The designed wind tunnel has 2.3 m in length and 0.74 m in height. Fig. 2 shows the final design of the structure.

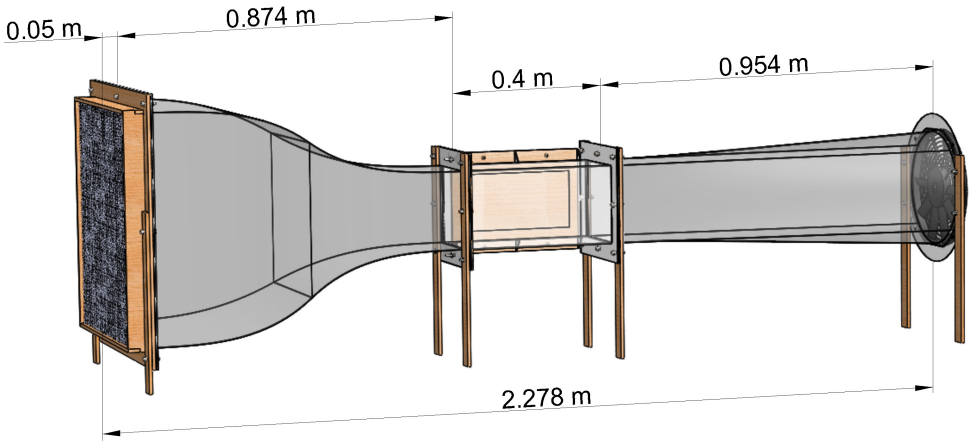

Figure 2. Wind tunnel 3D model

The settling chamber has a honeycomb screen made of aluminum alloy 3003H18. It has 0.58 m by 0.58 m in size and 0.04 m in thickness. The screen consists of 14355 cells. The cell wall thickness is $0.05 \cdot 10^{-3}$ m, and the size of a single cell is $5.2 \cdot 10^{-3}$ m.

The acrylic test section is transparent for the visualization of the experiments. This square section structure has a hydraulic diameter of 0.2 m and a length of 0.4 m. The test section has an opening of 0.3 m by 0.15 m to allow access from the outside of the tunnel. Fig. 3 represents the test section design.

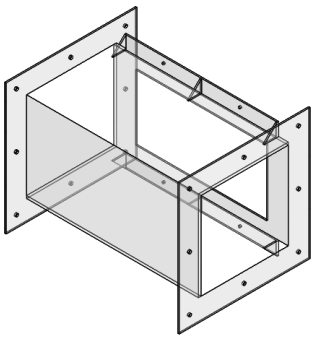

Figure 3. Test section

According to Barlow *et al.* (1999), the speed of 8.94 m/s requires a fan power of more than 17.6 W. The closest 0.3 m fan found on the market for this project is the straight-bladed biphasic fan of 80 W controlled by a Pulse-Width Modulation (PWM) signal. A commercial axial fan is installed in the circular part of the diffuser (Fig. 2). To control the fan rotation and consequently the flow speed, the PWM has a potentiometer that, when rotated, increases or decreases the fan speed.

The experimental investigation with the tachometer and anemometer allowed determining the flow speed after the fan and the RPM as a function of flow velocity. Table 1 and Figure 4 show the rotation speed, velocity, and dynamic pressure.

As mentioned earlier, the acceptable inlet-to-outlet area ratio lies between 8 and 9 Ahmed (2013). Thus, with an inlet

Table 1. Experimental study of the fan

Position of the potentiometer (%)	**RPM**	**V (m/s)**	**Pressure (Pa)**
12.5	133 ± 34	$0 + 0.24$	0
25	602 ± 25	2.35 ± 0.30	3.27
37.5	937 ± 29	3.85 ± 0.24	8.78
50	1209 ± 15	5.1 ± 0.25	15.41
62.5	1518 ± 17	6.1 ± 0.39	22.05
75	1787 ± 27	7.4 ± 0.26	32.45
87.5	2070 ± 20	8.2 ± 0.34	39.84
100	2219 ± 10	9.4 ± 0.34	52.35

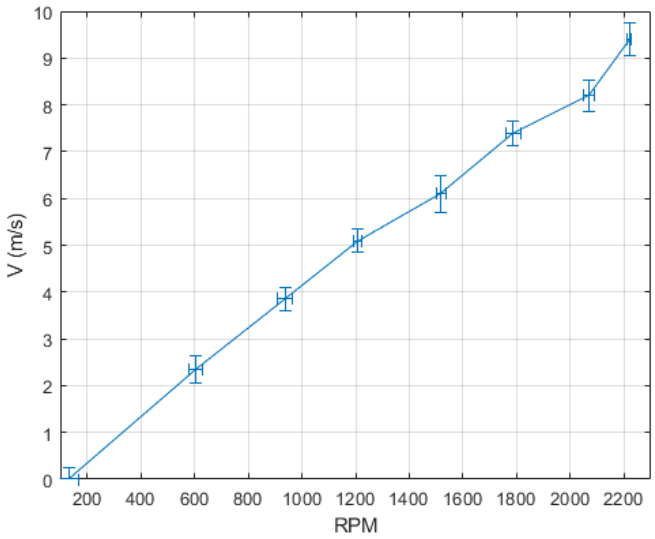

Figure 4. Speed vs. revolutions per minute (RPM)

of 0.58 m X 0.58 m and an outlet of 0.2 m X 0.2 m, the contraction ratio is 8.41. Accounting for the inlet dimension and respecting the $\alpha/2$ and $\beta/2$ angles of 12°, the nozzle length is 0.874 m according to the equation 3. Another critical factor is the shape of the nozzle defined by two equations of the third order that form the nozzle shape. The left view of Fig. 5 presents the final geometry of the inlet diffuser.

From the defined fan diameter and using the equation 3, the diffuser length is 0.974 m. The inlet region is square (Fig. 5) and has dimensions of 0.2 m by 0.2 m. The exit section of the diffuser has a diameter of 0.3 m. The area ratio between the circular and square sections is 1.75.

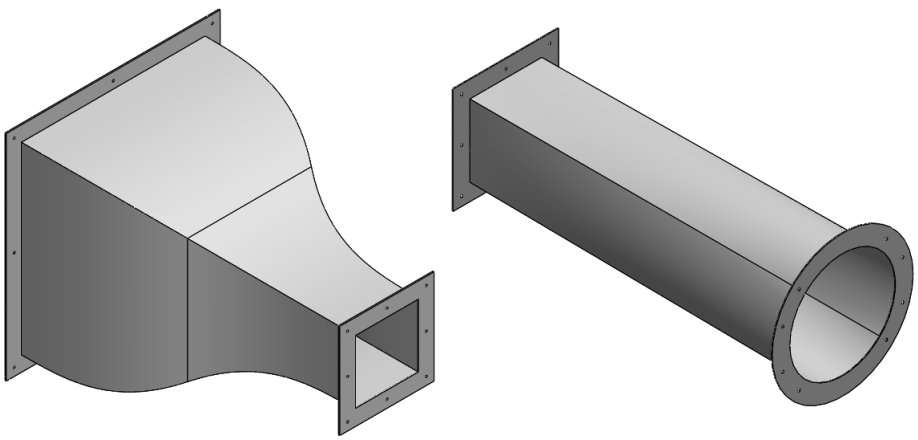

Figure 5. Nozzle and diffuser

3.2 Numerical results

3.2.1 Computational domain

The simplified geometry presented in Figure 6 shows the computational domain. Here, removing all the gaps and the flow straightener and assuming the uniform flow at the tunnel entrance, the flow domain was established. The geometry of the tunnel has vertical and horizontal symmetry axes, and the computational volume consists only of the quarter of the tunnel (Fig. 6) —such a solution allows significantly reducing computational requirements.

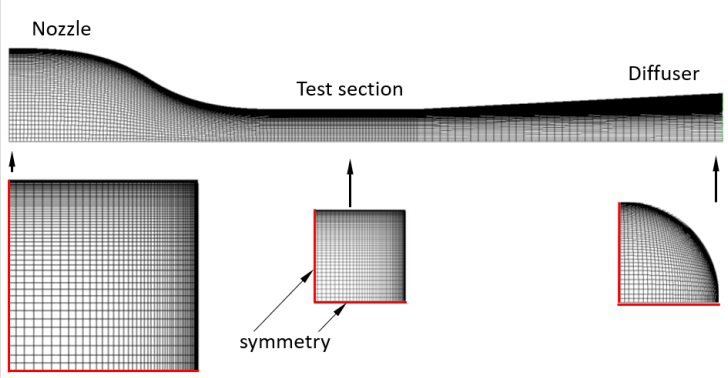

Figure 6. Computational domain and mesh

3.2.2 Mesh

The curvilinear structured mesh generation follows the Ansys Verification Models (AVM) manual Ansys (2020). It establishes the meshing properties to achieve a valid simulation result. The mesh consists of 160 divisions in the axial direction (X-axis) uniformly distributed along the axis: 80 cells in the nozzle, 40 in the test section, and 40 in the diffuser. There are 50 horizontal (Y-axis) and vertical (Z-axis) divisions, having the bias factor of 20.0 to account for the boundary layer effect. Constructed mesh (Fig. 6) consists of 400,000 elements and satisfies the AVM requirements, and consequently does not require further validation.

3.2.3 Simulation Results

According to the methodology described in section 2.2, and defining the ventilator pressure drop of 30 Pa as a boundary condition and constant velocity of 10 m/s as initial conditions, the simulation project has been calculated. The convergence of residuals happened after 80 simulation steps. Analysis of the results showed the following. The flow pattern is smooth, following the wall without the flow separation. Figure 7 presents the velocity distribution. When a viscous flow meets a flat plate, the formation of boundary layer happens, divided into two regions, the laminar and the turbulent. Knowing the thickness of the boundary layer analytically is important for validation of numerical simulations. The thin turbulent boundary layer has a predicted structure by analytical model Anderson (2016).

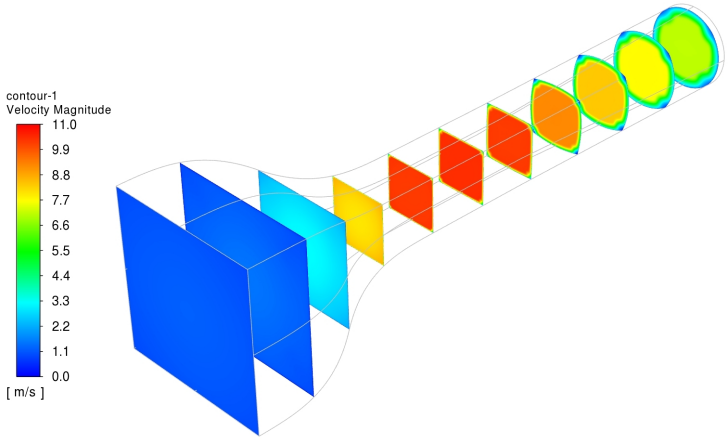

Figure 7. Velocity distribution along the wind tunnel

Analysis of the boundary layer behavior presented in Figure 8 shows a reasonable thickness of the boundary layer. It

occupies nearly 5% of the crossectional area at the inlet of the test section and approximately 9% at its exit. At the same time, a uniform velocity distribution outside of the boundary layer justifies the nozzle and diffuser design.

The pressure plot presented in Figure 8 shows the change o the static pressure in the test section along the axis, from 0 to 400 mm, and in the perpendicular direction to the wall. According to collected data, the pressure change in the axial direction happens due to the flow acceleration because of the boundary layer growth and friction with the wall. Additionally, pressure changes excessively at the end of the test section (x = 0.4 m) near the entrance to the diffuser, adapting the flow to the growth of the crossectional area.

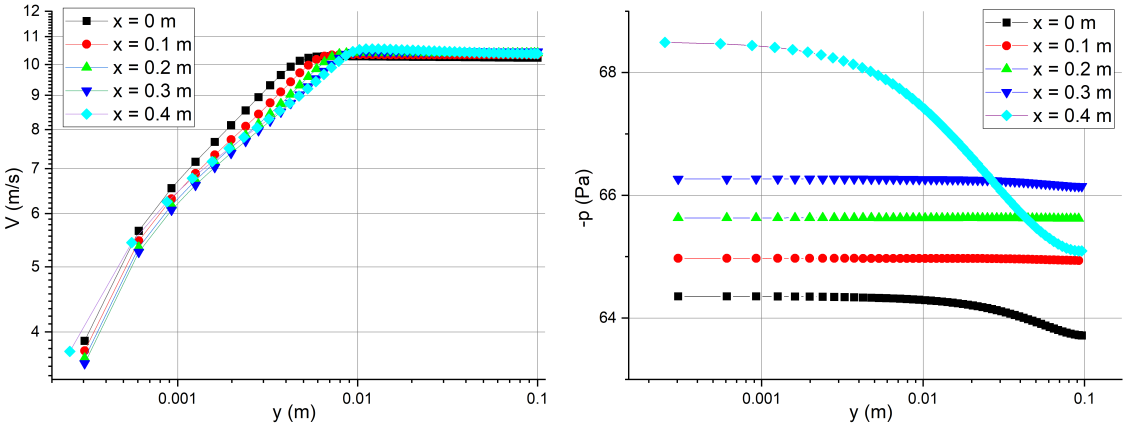

Figure 8. Velocity and pressure profiles in the test section of the wind tunnel

4. CONCLUSIONS

The authors defined the dimensions and shape of the low-velocity didactic open-circuit wind tunnel. The length of the tunnel is 2.3 m. The square test section is transparent and has the size of 0.4 m x 0.2 m x 0.2 m. The tunnel components are designed to provide a highly uniform flow in the test section and are compatible with the equipment available on the market: fan, sensors, fog machine. The numerical simulation showed that the nozzle effectively accelerates the flow and the boundary layer occupies from 5% to 9% of the test section. The uniform velocity profile in the test region is favorable for experimental aerodynamics.

Future development will focus on constructing the test bench structure, assembling and experimental study of the tunnel properties, CFD analysis to characterize turbulence levels in the test section, and finally, testing aerodynamic systems and flow visualization. Exploratory testing and flow simulation validated by tests will play an essential role in studying applied aerodynamic problems.

5. ACKNOWLEDGEMENTS

6. REFERENCES

Ahmed, N.A., ed., 2013. *Wind Tunnel Designs and Their Diverse Engineering Applications*. Janeza Trdine 9, 1st edition.

Anderson, J.D., 2016. *Fundamentals of Aerodynamics*. McGraw-Hill, 6th edition.

Ansys, 2020. *ANSYS Fluid Dynamics Verification Manual*. ANSYS, Inc.

Barlow, J.B., Rae, W.H. and Pope, A., 1999. *Low-Sppeed Wind Tunnel Testing*. John wiley Sons, Inc., 3rd edition.

Bitzer, T., 1997. *Honeycomb Technology*. spring-Science+Business Media, B.V., 1st edition.

Carminatti, L.J. and Konrath, R., 2019. "Desenvolvimento de um túnel de vento subsônico com foco no ensino didático". *Anais Engenharia Mecânica UCEFF*, Vol. 4, No. 1, pp. 1–17.

Driss, Z., ed., 2019. *Wind Tunnels Uses and Developments*. Nova Science publishers, Inc, 1st edition.

Mehta, R.D. and Bradshaw, P., 1979. "Tecnichal notes: Design rules for small low speed wind tunnels". *The Aeronautical Journal of The Royal Aeronautical Society*.

Tannehill, J.C., Anderson, D.A. and Pletcher, R.H., 1997. *Computational Fluid Mechanics and Heat Transfer*. Taylor Francis, 2nd edition.

Zanoun, E.S., 2018. "Flow characteristics in low-speed wind tunnel contractions: Simulation and testing". *Alexandria Engineering*, pp. 2265–2277.

7. RESPONSIBILITY NOTICE

The author(s) is (are) solely responsible for the printed material included in this paper.